

UNCERTAINTY QUANTIFICATION OF NO_x EMISSIONS INDUCED THROUGH THE PROMPT ROUTE IN PREMIXED ALKANE FLAMES

Antoine Durocher
ASME Student Member
McGill University
Montréal, Canada

Philippe Versailles
ASME Member
McGill University
Montréal, Canada

Gilles Bourque
ASME Fellow
Combustion Key Expert
Siemens Canada Limited

Jeffrey M. Bergthorson*
ASME Member
Associate Professor
McGill University
Montréal, Canada

Adjunct Professor
McGill University
Montréal, Canada

ABSTRACT

Increasingly stringent regulations on emissions in the gas turbine industry require novel designs to minimize the environmental impact of oxides of nitrogen (NO_x). The development of advanced low-NO_x technologies depends on accurate and reliable thermochemical mechanisms to achieve emissions targets. However, current combustion models have high levels of uncertainty in kinetic rates that, when propagated through calculations, yield significant variations in predictions. A recent study identified and optimized nine elementary reactions involved in CH formation to accurately capture its concentration and improve prompt-NO predictions. The current work quantifies the uncertainty on peak CH concentration and NO_x emissions generated by these nine reaction rates only, when propagated through the San Diego mechanism. Various non-intrusive spectral methods are used to study atmospheric alkane-air flames. 1st- and 2nd-order total-order expansions and tensor-product expansions are compared against a reference Monte Carlo analysis to assess the ability of the different techniques to accurately quantify the effect of uncertainties on the quantities of interest. Sparse grids, subsets of the full tensor-product expansion, are shown to retain the advantages of tensor formulation compared to total-order ex-

pansions while requiring significantly fewer collocation points to develop a surrogate model. The high resolution per dimension can capture complex probability distributions witnessed in radical species concentrations. The uncertainty analysis of lean to rich flames demonstrated a high variability in NO_x predictions reaching up to 400 % of nominal predictions. Wider concentration intervals were observed in rich conditions where prompt-NO_x is the dominant contributor to emissions. The high variability and scale of uncertainty in NO_x emissions originating from these nine elementary reactions demonstrate the need for future experiments and data assimilation to constrain current models to accurately capture CH for robust NO_x emissions predictions.

INTRODUCTION

Nitrogen oxides (NO and NO₂, labelled NO_x) are primary pollutants in the atmosphere, responsible for environmental and human health problems. New combustion technologies developed to achieve higher efficiency in industrial gas turbines must also reduce pollutants emissions. Increasingly accurate models and predictions are then required to identify and rank these promising designs [1].

Various complex thermochemical mechanisms tailored for specific applications have been developed to capture NO_x emis-

*Corresponding author. Email: jeff.bergthorson@mcgill.ca

sions [2]. Combustion kinetics research has identified and discussed four NO_x production routes for gaseous hydrocarbon combustion: prompt (Fenimore), thermal (Zel'dovich), N₂O, and NNH [3]. Post-flame pathways in high temperature zones motivated research, such as WLE and DLE combustion systems, to reduce the thermal NO_x contribution [4, 5]. Yet, emissions reductions in the flame front are limited by the presence of the flame. This motivated research in fuel-lean operating conditions and biofuels to mitigate the impact of flame front NO_x production, such as prompt-NO_x formation [6, 7].

An extensive series of NO and CH concentrations, as well as temperature and velocity profiles, have recently been published for lean to rich flames of C₁-C₄ alkane and alcohol fuels [8–10]. The atmospheric jet-wall stagnation flames showed a fuel-independent linear relationship between the rapid prompt-NO formation, and the peak concentration of methylidyne radical, [CH]_{peak}, scaled by the characteristic residence time in the CH layer, indicating that CH formation can be described by fuel-independent elementary reactions. A wide variability in CH predictions was observed for various known thermochemical mechanisms, where none of the proposed models were able to accurately capture quantitative absolute [CH]_{peak} measurements obtained with Laser-Induced Fluorescence (LIF) [10]. These inconsistencies were found to hinder the ability to predict prompt-NO formation, hence NO_x concentration. Versailles et al. subsequently showed that optimizing only nine CH-sensitive and uncertain reactions in the San Diego mechanism [11] reconciled predictions with CH-LIF measurements for C₁-C₃ fuel-air mixtures with ϕ ranging from 0.7 to 1.5 [12].

Uncertainty analysis has been recognized as a necessary effort in any modelling attempt in combustion chemistry development to quantify the impact of model inaccuracies [13, 14]. Recently, it was used to propagate parametric uncertainties to obtain probable intervals on predictions [15], constrain prior distributions with experimental data [16], and optimize mechanisms under uncertainty with PrImE [17]. Historically, computationally expensive sampling methods and response surfaces were used to systematically treat the uncertainty of kinetic parameters [18, 19]. The introduction of non-intrusive spectral methods, stemming from the work of Wiener [20], provides an inexpensive strategy to capture non-linear effects [21], and to perform optimization under uncertainty to provide constrained models for the community [16]. Using a Monte Carlo approach, Zsély and co-workers identified the prompt-NO route as a major contributor to uncertainty in NO concentration for lean to rich flames [19]. They observed that uncertainty in kinetic rates, rather than heats of formation, were responsible for the uncertainties in NO concentrations. Similar results were found in [22, 23] for mixtures diluted with exhaust gas components using linear sensitivity methods.

The current paper aims to identify an optimal uncertainty quantification technique applicable to combustion kinetics to quantify the uncertainties on [CH]_{peak} and prompt-NO_x arising

from the nine most CH-sensitive and uncertain reactions identified in [12]. Non-intrusive polynomial chaos expansions are used to investigate C₁-C₃ atmospheric alkane-air flames. The spectral techniques studied are: (1) total-order expansion, (2) tensor-product expansion, and (3) sparse grids. These spectral techniques are compared to Monte Carlo simulations to identify an optimal method to quantify the inherent uncertainties in mechanisms for robust emissions predictions.

METHODOLOGY

Response surfaces have been previously used to optimize thermochemical mechanisms against experimental data sets [18]. The surfaces generated provide an economic approach to quantify uncertainties and perform optimization in combustion problems since complex systems are expressed by algebraic equations. The entire space of parameters and operating conditions can then be sampled at relatively low cost. Generating an accurate response surface has traditionally been an expensive process involving stochastic techniques. Introduction of spectral methods, also known as polynomial chaos expansions (PCE), enables response surface mapping at a fraction of the cost of sampling techniques, and provides the opportunity to study complex combustion phenomena with accurate treatment of uncertainties.

In this work, a framework is developed to assess the impact of parametric uncertainties propagated through the San Diego mechanism [11], using the 2004-v2 nitrogen chemistry with the 2005 base chemistry. Figure 1 presents the work flow combining direct one-dimensional flame simulations with Cantera 2.3 [24], streamlined with Dakota 6.6 [25] to perform uncertainty analyses. The Dakota package offers a variety of uncertainty techniques, including sampling and spectral methods, to study the impact of the choice of method on the accuracy of the generated response surface. The framework consists of three core sections. (1) The uncertain kinetic space, bounded by values found in the literature, is sampled using random or structured collocation points. The sampled reaction rates are then imported to one-dimensional flame simulations. The process is repeated until the number of evaluations required to calculate the coefficients of the expansion is reached. (2) Using the detailed complete solutions from direct simulations, the coefficients of the spectral expansion are evaluated to provide surrogate models. (3) The surrogate model, or polynomial expansion, can then be randomly and exhaustively sampled over the entire uncertain space to obtain probability distribution of the quantities of interest and provide numerical “error bars” on predictions.

Uncertainty limits must first be identified for the reactions studied to provide reasonable bounds for the analysis. Only pre-exponential factors are considered in the analysis as they were shown to have the greatest influence [12, 19, 23]. The uncertainties of the pre-exponential coefficient, the temperature exponent, and the activation energy are effectively lumped to provide un-

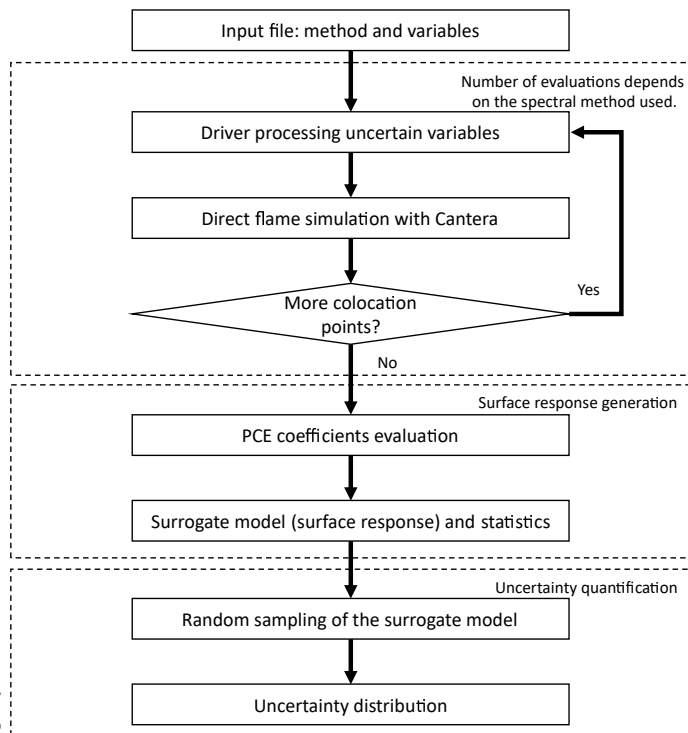


FIGURE 1. UNCERTAINTY QUANTIFICATION FRAMEWORK USING DIRECT FLAME SIMULATIONS FOR SURROGATE MODEL CONSTRUCTION.

certainty limits on the kinetic rate. A multiplier can then be applied on the nominal reaction rate.

Identification of parameters and distributions

Logarithmic sensitivities for $[\text{CH}]_{\text{peak}}$ were first obtained for $\text{C}_1\text{-C}_3$ fuels over equivalence ratios ranging from 0.7 to 1.5. Reaction uncertainty factors were then multiplied with logarithmic sensitivities to obtain an uncertainty-weighted sensitivity index. The nine reactions with the highest index, shown in Table 1, correspond to the reactions identified in [12] and are used to perform the uncertainty analysis. The uncertainty on kinetic reaction rates is typically presented in terms of $\Delta \log_{10} k_i$ for the i^{th} reaction. The bounds on reaction rates are provided as uncertainty factors $f_i = 10^{\Delta \log_{10} k_i}$ that are multiplied with nominal rates to perform the analysis. The definition of uncertainty limits follows the work of Versailles et al., with probable and physically realistic intervals found in [26–28]. The relative errors are expressed as follows.

$$\left. \frac{\Delta k_i}{k_i} \right|_{\text{low}} = \frac{k_i/f_i - k_i}{k_i} = \frac{1}{f_i} - 1 \quad (1)$$

$$\left. \frac{\Delta k_i}{k_i} \right|_{\text{high}} = \frac{k_i \cdot f_i - k_i}{k_i} = f_i - 1 \quad (2)$$

The resulting asymmetric uncertainty bands retain the mechanism properties, obtained through model optimization with multiple targets, while satisfying preferred physically realistic uncertainty limits. Known relationships between uncertain parameter distributions and polynomial bases have been studied in statistics [29]. To benefit from known bases, such as Legendre polynomials, the uncertain rate parameters are normalized over the uncertainty interval, taking values between $[-1, 1]$. Since experimental results are too scarce to derive any significant statistics from previous reaction rate measurements, uniform prior distributions are used to avoid bias. Additional measurements would be required to constrain the parameter space and identify a different prior probability distribution.

Uncertainty quantification techniques

Uncertainties have traditionally been quantified with stochastic (Monte Carlo) sampling techniques [19,30]. Response surfaces could be fitted to multiple evaluations to perform model optimization against experimental data [18]. The spectral expansion, introduced by Wiener [20], was shown to be an economic alternative to perform uncertainty analyses for combustion systems [13, 16]. Yet, it suffers from the curse of dimensionality as the required number of collocation points increases exponentially with the number of input parameters studied. This paper examines various uncertainty quantification techniques for fast and optimal predictions of quantities of interest. A Monte Carlo method using Latin hypercube sampling (LHS) provides reference $[\text{CH}]_{\text{peak}}$ and prompt- NO_x distributions. 1st- and 2nd-order polynomial expansions are then used to assess the accuracy of traditional expansion techniques. Tensor-product expansions with 2nd-order polynomials and sparse grid methods are studied as alternatives for high-dimensional multivariate problems.

Monte Carlo and advanced sampling techniques, such as Latin hypercube sampling shown in Fig. 2a, provide an intu-

TABLE 1. UNCERTAINTY BOUNDS, $1/f_{i,\text{low}}$ AND $f_{i,\text{high}}$.

Reactions	$1/f_{i,\text{low}}$	$f_{i,\text{high}}$
$\text{CH} + \text{O}_2 \leftrightarrow \text{HCO} + \text{O}$	0.4747	2.456
$\text{CH}_2 + \text{OH} \leftrightarrow \text{CH} + \text{H}_2\text{O}$	0.2409	2.168
$\text{CH}_2 + \text{H} \leftrightarrow \text{CH} + \text{H}_2$	0.7579	127.6
$\text{H} + \text{CH}_3(+\text{M}) \leftrightarrow \text{CH}_4(+\text{M})$	0.2577	3.246
$\text{CH}_3 + \text{OH} \leftrightarrow \text{CH}_2^* + \text{H}_2\text{O}$	0.3653	2.324
$\text{CH} + \text{H}_2\text{O} \leftrightarrow \text{CH}_2\text{O} + \text{H}$	$3.823 \cdot 10^{-2}$	5.295
$\text{CH}_2 + \text{O}_2 \leftrightarrow \text{CO} + \text{OH} + \text{H}$ $\leftrightarrow \text{CO}_2 + \text{H}_2$	0.8482	8.482
$\text{CH}_2\text{CO} + \text{O} \leftrightarrow \text{CH}_2 + \text{CO}_2$	$5.808 \cdot 10^{-3}$	1.502

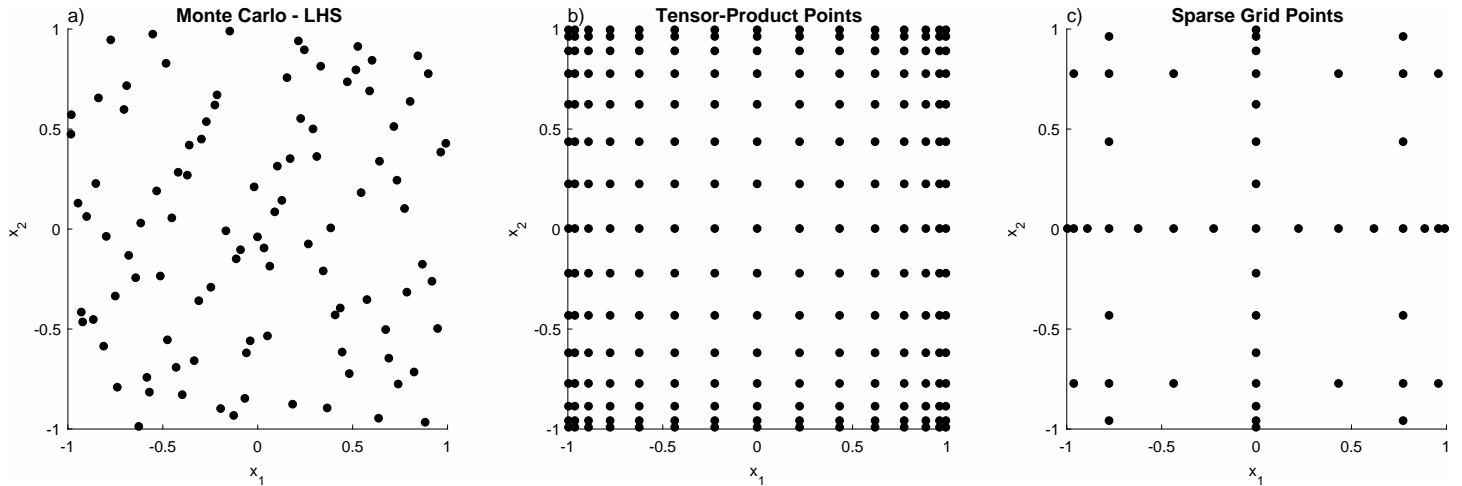


FIGURE 2. COLLOCATION POINTS USED TO EVALUATE THE COEFFICIENTS IN A SPECTRAL EXPANSION OF TWO VARIABLES. a) MONTE CARLO - LHS. b) TENSOR-PRODUCT USING GAUSS-PATTERSON. c) SPARSE GRID USING GAUSS-PATTERSON, THE ACCURACY ON A PER-DIMENSION BASIS IS MAINTAINED.

itive way to assess numerical uncertainties. Provided that enough randomly distributed samples are evaluated, the solution should approach the true distribution based on the law of large numbers. Stochastic sampling techniques generally require minimal modifications to existing numerical tools to cover the parameter space. They are independent of the dimensions of the problem since the entire space can be sampled simultaneously, but suffer from major drawbacks: (1) they show slow convergence, hence high computational costs; and (2) they only provide moments of the statistical distributions of interest and do not identify the relationship between parameters.

Spectral methods address some of the shortcomings of sampling techniques. Fewer evaluation points are needed to constrain surrogate models used for uncertainty quantification, optimization, and inference. Additionally, they provide parameter interactions and offer the opportunity to sample subset of the surrogate model. For these reasons, stochastic spectral methods have been gaining popularity and have followed an intense period of development [31, 32].

Polynomial chaos expansion is based on the assumption that a given response can be expressed as an infinite series of multivariate polynomials. Practically, the series is truncated to the desired order p , resulting in high-order approximations of multivariate phenomena. In other words, spectral expansion relates the quantity of interest R to the n -element vector of uncertain parameters \mathbf{x} using the compact notation:

$$R(\mathbf{x}) \approx \sum_{k=0}^K \alpha_k \prod_{i=1}^n \psi_{t_i^k}(x_i), \quad (3)$$

where α_k is the k^{th} coefficient in the expansion, $\psi_{t_i^k}$ is the one-dimensional polynomial of the i^{th} uncertain variables, and t_i^k matches the desired polynomial order of the k^{th} term for the variable i . In traditional total-order expansions, the resulting response surface has a maximum polynomial order of p , where the total number of terms K in Eq. 3 can be expressed as:

$$K = \frac{(n+p)!}{n!p!}. \quad (4)$$

The number of terms K defines the required number of evaluations to constrain the calculation of coefficients. Using randomly selected collocation points (Fig. 2a), polynomial coefficients can then be evaluated through linear regression, or extracted from orthogonal projections on each basis function. Although this approach uses random sampling similar to Monte Carlo, it requires fewer sample points as it uses predetermined polynomials to evaluate coefficients.

Alternatively, structured grids (Fig. 2b and c) can be used instead of random points to ensure systematic coverage of the uncertain space. Tensor-product expansions (Fig. 2b) use structured grids with known weights and integration points to evaluate polynomial coefficients, instead of random collocation points. In this approach, the bound on the polynomial order is defined per dimension, or variable, and not on the total expansion. Hence the combination of all one-dimensional polynomials yields a total polynomial order of $p \times n$. To constrain the coefficients, the

number of evaluations required for this expansion is:

$$K = \prod_{i=1}^n (p_i + 1), \quad (5)$$

where the n and p_i represent the number of uncertain variables studied and the polynomial order of the i^{th} basis, respectively. The tensor-product expansion suffers from the curse of dimensionality more severely than traditional total-order expansion. Hence, it is not recommended for analyses with large numbers of parameters. An advantage of tensor-product formulation is that it supports anisotropic expansion, where the polynomial order can be different on a per-variable basis to increase the resolution of specific parameters.

Sparse grids were proposed by Smolyak [33] to provide similar accuracy as tensor-product expansions with significantly fewer quadrature points. The approach includes only a subset of the full expansion by removing multivariate high-order terms from the expansion. Figure 2c shows a sparse grid extracted from the two-dimensional tensor-product expansion presented in Fig. 2b. The resolution on a per-dimension basis is conserved, while correlation points between the two variables are reduced to remove higher order interactions in the expansion. The resulting grid can then provide high polynomial accuracy per dimension, while still capturing 1st- or 2nd-order cross-correlation effects between parameters.

The choice of quadrature method and level of accuracy required in sparse grids affect the number of evaluation points, and no simple and unique formula for the required number of points is available. Examples in [32] show significant reduction in calculation costs for various problems with high-dimensionality. For instance, a problem with 50 parameters and a 5th-order expansion would require 5101 points using sparse grids and over 8×10^{34} evaluations with a tensor-product expansion. For comparison, a total-order expansion with lower resolution would require 3.5×10^6 random evaluations to constrain the coefficients, and a Monte Carlo analysis could require 1×10^8 evaluations for similar accuracy.

RESULTS

The impact on $[\text{CH}]_{\text{peak}}$, NO_x , and reference flame speed, S_u , caused by parametric uncertainties for atmospheric $\text{C}_1\text{-C}_3$ alkane fuel-air mixtures were quantified for the nine reactions in Table 1. To account for different flame positions caused by the varying flame speed, NO_x concentrations are taken 1 ms after the $[\text{CH}]_{\text{peak}}$ to systematically compare emissions.

The quantities of interest are studied with 5 techniques to assess their ability to accurately capture the distribution of a ref-

erence Monte Carlo method with 4000 evaluations. Legendre polynomials are used as bases to develop the response surfaces since uniform prior distributions are used. Total-order expansion is used to investigate traditional uncertainty quantification techniques used in combustion with (1) a 1st-order expansion with the minimum number of collocation points, (2) a 2nd-order expansion with the minimum number of collocation points, and (3) a 2nd-order expansion with four times the minimum number of collocation points. Tensor-product expansion is applied for a (4) 2nd-order expansion and (5) a level 2 sparse grid with a nested Gauss-Patterson quadrature rule to assess the accuracy of structured grids for combustion phenomena.

Additionally, nominal solutions of known mechanisms used in industrial gas turbine applications are compared to the uncertainty distributions to verify that they fall within the most probable interval obtained from uncertain numerical predictions. For the purpose of this study, the last version of the thermochemical mechanism developed through the effort of the Gas Research Institute, GRI-Mech 3.0 (GRI) [34], and the 2005 version of the San Diego mechanism (SD) [11] with NO_x chemistry are used to assess the accuracy of two small detailed mechanisms widely used in the industry for emissions predictions.

Method Accuracy

The distributions of the five uncertainty quantification techniques are shown in Fig. 3 against the Monte Carlo distributions. A selection of lean to rich mixtures of fuels from methane to propane is shown to illustrate the ability of the methods to capture various features of flames with significantly different uncertainty distribution shapes. Furthermore, distribution means and standard deviations are given in Table 2 for methane only.

Every technique studied produces reasonable estimates of the statistics for the three quantities of interest, as shown in Table 2. The simplest 1st-order approximation captures relatively well the average value of the distributions and the standard deviations. Without a Monte Carlo analysis to provide probability distributions, and only looking at the first two moments, any of the techniques studied would appear to be a good option. However, upon detailed inspection of the distribution shown in Fig. 3, all techniques are not equal.

Traditional total-order expansion techniques with 1st- and 2nd-order polynomials show their inability to fully capture the distribution profiles of all the quantities of interest studied. As expected, the 1st-order expansion does not capture the actual shape of the distributions as it uses the simplest response surface, and it provides significantly wider distributions. The large distribution tails can extend to negative concentrations caused by approximation errors in the regression to build the surrogate model. These negative concentrations are physically impossible, and are clearly shown by the sharp Monte Carlo distribution at 0 ppm. The 2nd-order total-order expansion better captures the

TABLE 2. AVERAGE AND STANDARD DEVIATION COMPARISON OF PCE TECHNIQUES FOR METHANE-AIR MIXTURE ($\phi = 0.9$).

Method	CH peak (ppm)		NO _x (ppm)		S _u (m/s)	
	Average	Std. Deviation	Average	Std. Deviation	Average	Std. Deviation
MC-LHS (4000 points)	1.563	1.494	22.43	8.107	0.3384	0.02967
1 st -order total-order (9 points)	1.539	1.144	21.16	6.029	0.3399	0.02821
2 nd -order total-order (45 points)	1.568	2.000	22.49	11.54	0.3405	0.03547
2 nd -order total-order (180 points)	1.543	1.438	22.34	7.975	0.3402	0.03169
2 nd -order tensor-product (6561 points)	1.539	1.382	22.37	7.833	0.3400	0.02764
l ₂ sparse grid (161 points)	1.548	1.394	22.45	7.890	0.3464	0.03017

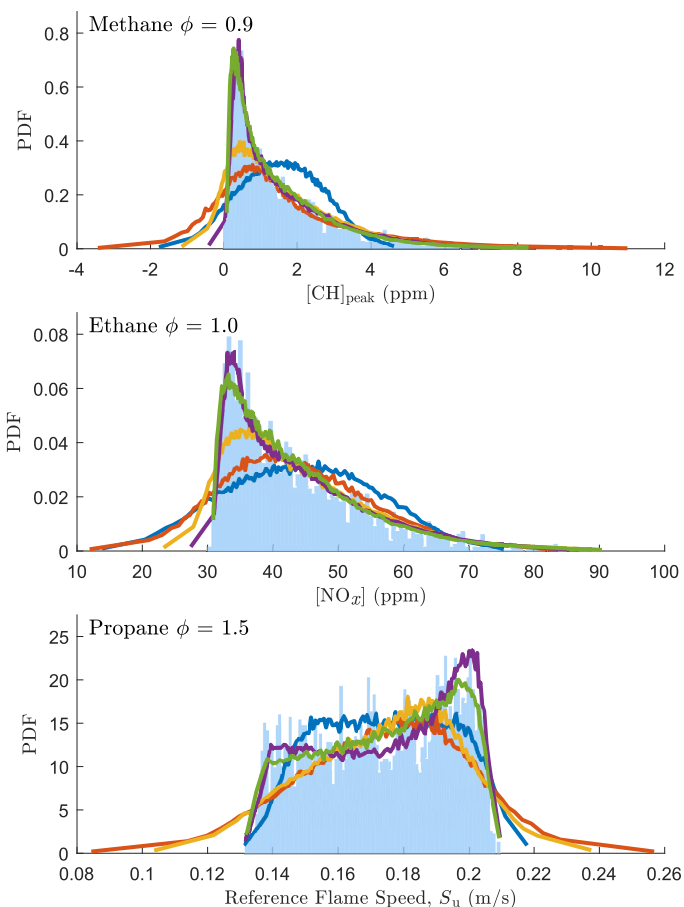


FIGURE 3. SPECTRAL METHODS COMPARISON TO MONTE CARLO SIMULATIONS FOR VARIOUS QUANTITIES OF INTEREST. ■: MONTE CARLO - LHS DISTRIBUTION (4,000 SAMPLES). TOTAL-ORDER EXPANSION WITH RANDOMLY DISTRIBUTED COLLOCATION POINTS, —: 1ST-ORDER (9 POINTS), —: 2ND-ORDER (45 POINTS), —: 2ND-ORDER (180 POINTS). STRUCTURED METHODS, —: l₂ NESTED SPARSE GRID USING GAUSS-PATTERSON QUADRATURE (161 POINTS), —: 2ND-ORDER TENSOR-PRODUCT (6561 POINTS).

peaks of $[\text{CH}]_{\text{peak}}$ and NO_x distributions, but is unable to capture more complex distribution shapes, as exhibited by the flame speed distributions. Increasing the number of collocations points used to calculate the coefficients, from the minimum number of 45 to 180 points, yield a more accurate response surface with tighter concentration distributions. It follows that the distribution shapes are better captured. The increased number of points allows a better mapping of the uncertain space and reduces the extrapolation error when the regression is performed to construct response surfaces. It better quantifies uncertainties, but the technique is still limited to the low-order approximation of a complex multi-physics phenomenon.

The higher-order approximation developed with a 2nd-order tensor-product expansion requires 6561 evaluations to fully constrain the expansion. The tensor product formulation is able to capture high-order interactions between multiple parameters since it does not limit the order of the total polynomial expansion. It accurately captures the distributions shown in Fig. 3 for the three targets, but represents a significant investment to perform complex multivariate simulations.

The alternative is to use only a subset of a tensor-product expansion, with sparse grids, to retain the accuracy while reducing the number of evaluations. The nested sparse grid requires 161 simulations, or collocation points, and accurately captures the peaks in $[\text{CH}]_{\text{peak}}$ and NO_x . The double-peaked distribution of laminar flame speed is captured and the width of the polynomial approximation is consistent with Monte Carlo sampling. With a comparable number of collocation points as the dense 2nd-order total-order expansion (180 points), the sparse grid technique exhibits more accurate approximations of the phenomenon. Contrary to the total-order expansion, sparse grids do not overestimate the tails of the distributions. As a result, they are considered the optimal compromise between accuracy and cost compared to tensor-product expansion.

Numerical uncertainties on predictions

The sparse grid methodology better captures the distributions of species concentrations, independently of fuel and operating conditions. For both $[\text{CH}]_{\text{peak}}$ and NO_x concentration, the dis-

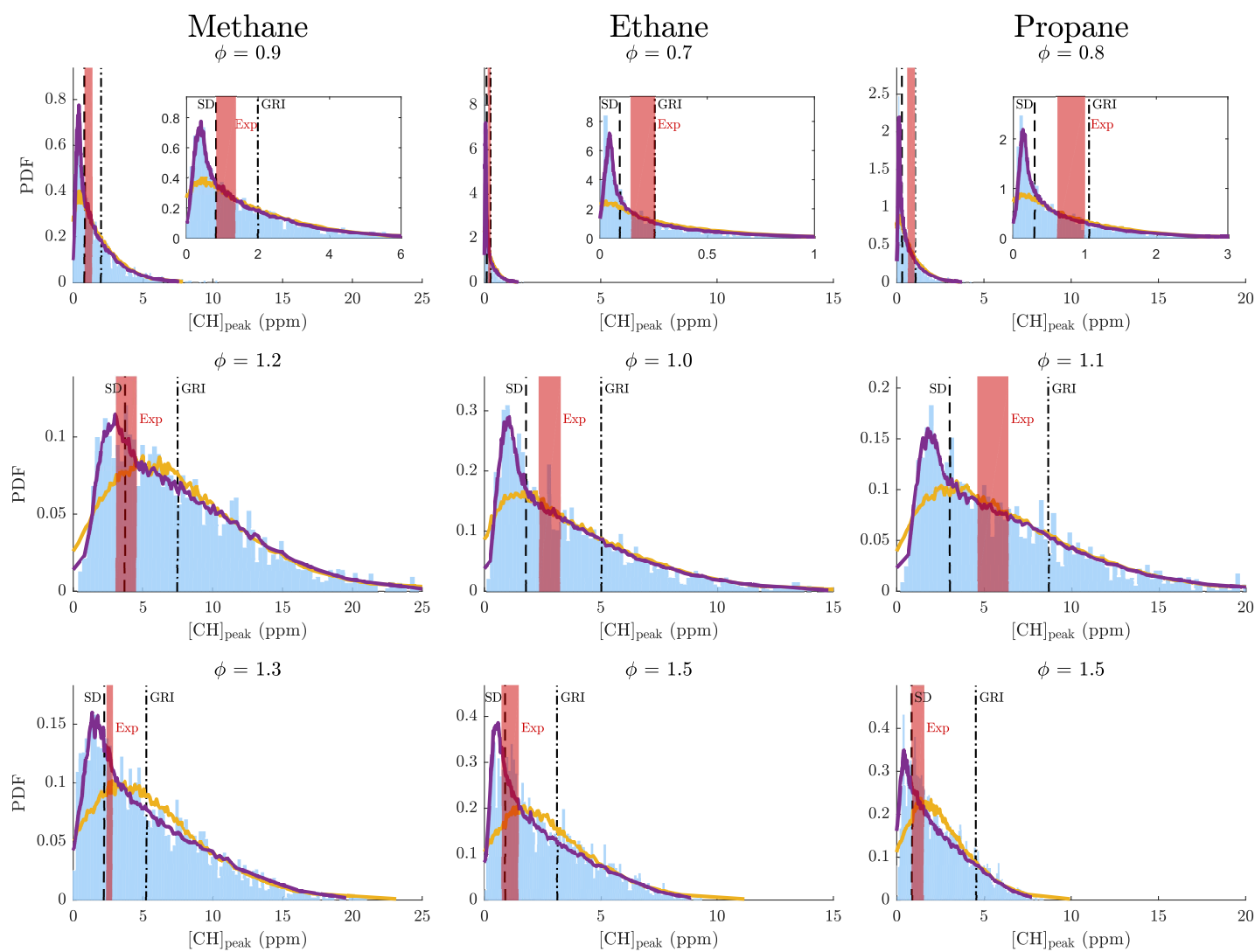


FIGURE 4. $[\text{CH}]_{\text{peak}}$ DISTRIBUTION FOR $\text{C}_1\text{-C}_3$ ALKANE-AIR MIXTURE. ■: MC-LHS (4,000 SAMPLES). ONLY POLYNOMIAL EXPANSIONS WITH SIMILAR NUMBER OF TERMS ARE SHOWN, —: 2nd-ORDER TOTAL-ORDER PCE (180 POINTS). —: l_2 NESTED SPARSE GRID PCE (161 POINTS). VERTICAL LINES ARE NOMINAL THERMOCHEMICAL MECHANISM RESPONSES FOR SD(- -) AND GRI(- - -). THE SHADED RED AREA (■) REPRESENTS THE EXPERIMENTAL RANGE MEASURED BY VERSAILLES AND CO-WORKERS [12].

tribution shapes are accurately identified with sparse grids. Retaining the advantages of tensor-product expansion, sparse grids provide high-order polynomials per variable to capture rapidly changing targets with the desired accuracy. For distributions with sharp features, such as CH concentration, a low-order response surface is not able to capture the shape, but can provide an approximation of the average value and standard deviation. However, traditional 2nd-order expansion techniques are still over-predicting the tails of the distributions.

In the following, only the sparse grids and 2nd-order total-order expansions (180 points) are shown in Figs. 4 and 5 for the

data set studied. Methods with a similar number of evaluations, or similar costs, are used to facilitate comparison between the accuracy of probability distributions.

The $[\text{CH}]_{\text{peak}}$ distributions in Fig. 4 are shown for $\text{C}_1\text{-C}_3$ alkane-air mixtures for lean (top) to rich conditions (bottom). Interestingly, the distribution width increases towards stoichiometric conditions before reducing slightly for rich conditions. The higher uncertainty in rich distributions compared to lean show that uncertain reaction rates in the CH route have a greater impact in stoichiometric and fuel rich conditions where prompt-NO_x is favoured. The width of stoichiometric distributions, predicting

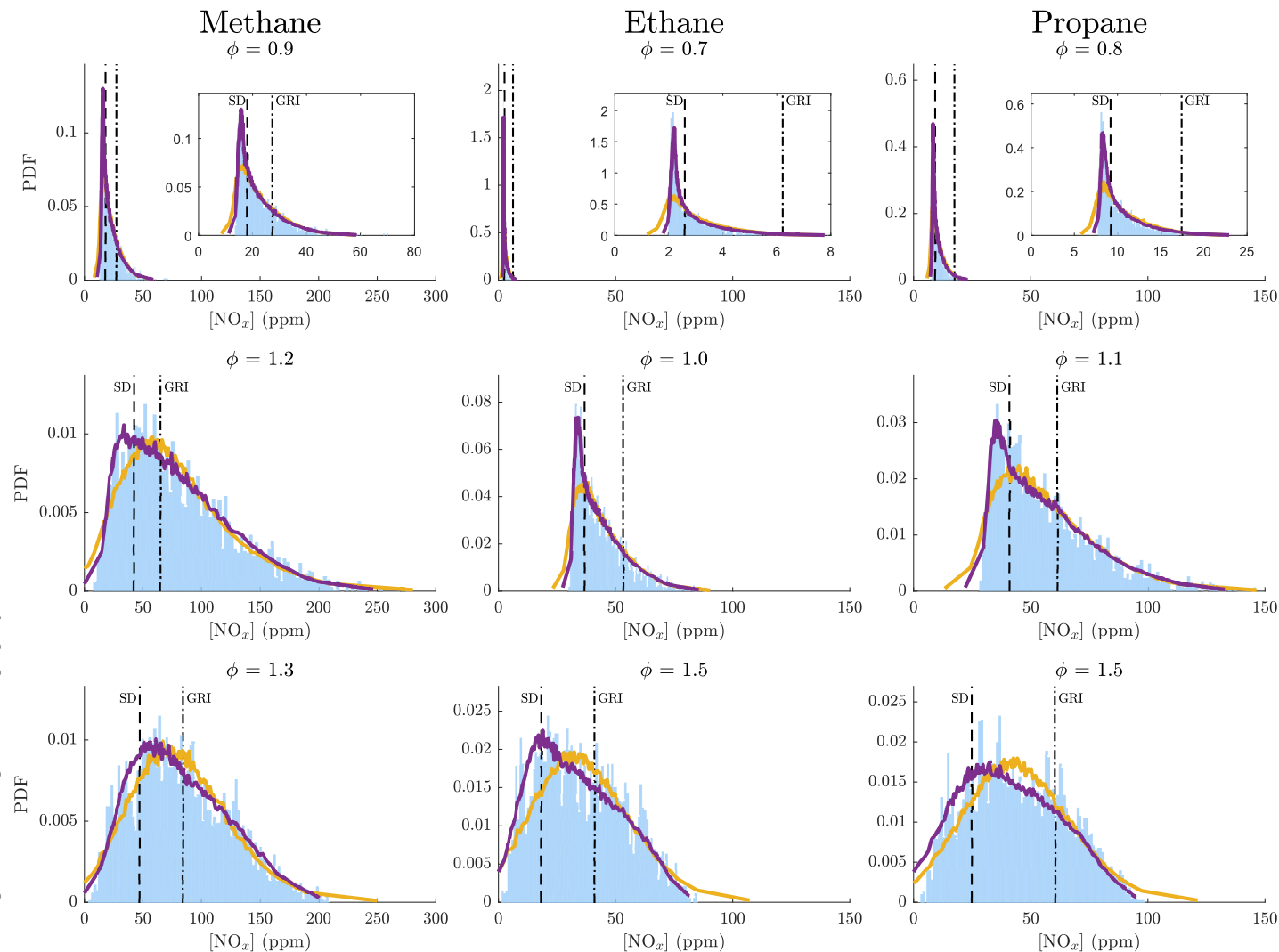


FIGURE 5. $[\text{NO}_x]$ DISTRIBUTION ATTRIBUTED 1 MS AFTER THE PEAK CH CONCENTRATION FOR ALKANE-AIR MIXTURE. ■: MC-LHS (4,000 SAMPLES). ONLY POLYNOMIAL EXPANSIONS WITH SIMILAR NUMBER OF TERMS ARE SHOWN, —: 2nd-ORDER TOTAL-ORDER PCE (180 POINTS). —: l_2 NESTED SPARSE GRID PCE (161 POINTS). VERTICAL LINES ARE NOMINAL THERMOCHEMICAL MECHANISM RESPONSES FOR SD(- -) AND GRI(- - -).

up to 400% of the nominal value, identifies the need for future experiments to constrain the uncertainty space of reactions involved in CH formation to enhance prediction accuracy.

Similar conclusions are obtained from the NO_x distributions shown in Fig. 5 for the same operating conditions. Studying only the nine CH-sensitive and uncertain reactions, a variation reaching up to 400% of nominal values is again observed in stoichiometric cases. The uncertainty in NO_x shown here is only caused by the prompt route initiated by the attack on nitrogen by CH radicals and is larger where the prompt mechanism dominates NO_x formation. The already large uncertainty in predictions is expected to increase with the addition of the other inherently un-

certain NO_x formation routes. As the equivalence ratio increases, it is interesting to note that distributions become smoother. The sharp peak with low concentration is absorbed and the 2nd-order polynomials are able to capture the distribution shapes.

The stoichiometric and rich distributions of NO_x show that greater uncertainty exists in predictions at those conditions. In gas turbine applications, where homogeneous near-perfect mixing is often sought, the impact of hot spots characterized by richer mixtures could, not only increase NO_x predictions, but also produce wider uncertainty bands on those predictions. Although the predictions of both mechanisms are within one standard deviation of the means, predictions with the San Diego

mechanism are generally below the average concentrations, resulting from the optimization performed during its development. For robust and accurate predictions to achieve emissions targets, a constrained description of uncertain reaction rates in the NO_x pathways is required. With the actual uncertainty attached to the kinetic rates, predicting which design can yield sub-10 vppm levels of NO_x with any confidence can be seriously questioned as the uncertainty in only nine reactions already produces a probable interval in NO_x predictions ranging over 100 ppm.

CONCLUSION

Uncertainties in CH and NO_x concentrations arising from nine CH-sensitive and uncertain elementary reactions identified by Versailles and co-workers [12] were quantified. The uncertainty in kinetic rates were propagated through the San Diego mechanism [11] with several techniques to provide accurate prediction intervals with minimal computational effort.

Sparse grid methods were identified as the most promising technique to accurately capture fast-radical formation with reasonable costs. Traditional total-order expansions using 1st- and 2nd-order polynomials showed limited accuracy, even with increased number of collocation points, when compared to Monte Carlo sampling. The over-prediction of distribution tails and misidentification of peaks showed that traditional uncertainty quantification strategies introduced significant modelling discrepancies in probability distributions of species concentrations. The reference Monte Carlo distributions could be reproduced with structured methods based on tensor-product expansion. Among them, sparse grid techniques benefited from the high-order expansion per dimension, which is necessary to capture complex distribution shapes, without the added contribution of high-order interactions between parameters. This approach demonstrated its capacity to accurately quantify uncertainties in numerical predictions, and is recommended for future uncertainty quantification and model optimization efforts.

The probability distributions of peak CH concentrations for C₁-C₃ alkane-air mixtures demonstrated that uncertainty limits from the literature, for only nine elementary reactions in the CH pathways, can currently allow for concentration predictions ranging between 0 and 25 ppm, corresponding to a variation of up to 400% from the nominal values. In comparison, experimental data only present uncertainties of approximately ±20%. This discrepancy between uncertainties in numerical predictions and experimental measurements highlights the need of future experiments to constrain the uncertainty of thermochemical mechanisms to, not only provide robust models to the combustion community, but also increase the confidence in predictions by reducing residual uncertainties.

As part of the prompt-NO_x pathway, uncertainties in the nine reactions also propagated through the NO_x sub-models to yield significant uncertainties in emissions predictions. Probable

prediction intervals, consistent with [CH]_{peak} distributions, cover similar relative concentration ranges up to 400% of nominal predictions. NO_x distributions demonstrate that, within chemically recommended limits, it is possible to tune a combustion model to completely suppress the prompt contribution to the total NO_x predictions, as shown by near-zero [CH]_{peak} and the 0 ppm NO_x concentrations of fuel-rich conditions that have a finite probability. Again, these findings reinforce the need of constrained mechanisms for accurate emissions predictions. Moving forward, emissions predictions should be given with uncertainty bands to reduce the risks associated with sub-10 vppm combustion technology development for gas turbine engines.

PERMISSION FOR USE

The content of this paper is copyrighted by Siemens Canada Ltd. and is licensed to ASME for publication and distribution only. Any inquiries regarding permission to use the content of this paper, in whole or in part, for any purpose must be addressed to Siemens Canada Ltd. directly.

ACKNOWLEDGMENT

The authors wish to acknowledge the support of the Natural Sciences and Engineering Research Council of Canada (NSERC), the Fonds de Recherche du Québec - Nature et Technologies and Siemens Canada Limited.

NOMENCLATURE

GRI	GRI-Mech 3.0 [34]
LHS	Latin hypercube sampling
PCE	Polynomial chaos expansion
SD	University of California, San Diego [11]

REFERENCES

- [1] Lieuwen, T., Chang, M., Amato, A., et al., 2013. "Stationary gas turbine combustion: Technology needs and policy considerations". *Combustion and Flame*, **160**(8), pp. 1311–1314.
- [2] Schofield, K., 2012. "Large scale chemical kinetic models of fossil fuel combustion: Adequate as engineering models - No more, no less". *Energy & Fuels*, **26**(9), pp. 5468–5480.
- [3] Miller, J. A., and Bowman, C. T., 1989. "Mechanism and modeling of nitrogen chemistry in combustion". *Progress in energy and combustion science*, **15**(4), pp. 287–338.
- [4] Göke, S., Schimek, S., Terhaar, S., Reichel, T., Göckeler, K., Krüger, O., Fleck, J., Griebel, P., and Paschereit, C. O., 2014. "Influence of pressure and steam dilution on NO_x

- and CO emissions in a premixed natural gas flame”. *Journal of Engineering for Gas Turbines and Power*, **136**(9), p. 091508.
- [5] Røkke, P. E., Hustad, J. E., Røkke, N. A., and Svendsgaard, O. B., 2003. “Technology update on gas turbine dual fuel, dry low emission combustion systems”. In ASME Turbo Expo 2003, collocated with the 2003 International Joint Power Generation Conference, American Society of Mechanical Engineers, pp. 97–107.
- [6] Bergthorson, J. M., and Thomson, M. J., 2015. “A review of the combustion and emissions properties of advanced transportation biofuels and their impact on existing and future engines”. *Renewable and Sustainable Energy Reviews*, **42**, pp. 1393–1417.
- [7] Correa, S. M., 1993. “A Review of NO_x Formation Under Gas-Turbine Combustion Conditions”. *Combustion Science and Technology*, **87**(1-6), pp. 329–362.
- [8] Watson, G. M., Versailles, P., and Bergthorson, J. M., 2016. “NO formation in premixed flames of C₁-C₃ alkanes and alcohols”. *Combustion and Flame*, **169**, pp. 242–260.
- [9] Watson, G. M. G., Versailles, P., and Bergthorson, J. M., 2017. “NO formation in rich premixed flames of C₁-C₄ alkanes and alcohols”. *Proceedings of the Combustion Institute*, **36**(1), pp. 627–635.
- [10] Versailles, P., Watson, G. M., Lipardi, A. C., and Bergthorson, J. M., 2016. “Quantitative CH measurements in atmospheric-pressure, premixed flames of C₁-C₄ alkanes”. *Combustion and Flame*, **165**, pp. 109–124.
- [11] University of California at San Diego, 2005. Chemical-kinetic mechanisms for combustion applications. <http://combustion.ucsd.edu>.
- [12] Versailles, P., Watson, G. M. G., Durocher, A., Bourque, G., and Bergthorson, J. M., 2017. “Thermochemical mechanism optimization for accurate predictions of CH concentrations in premixed flames of C₁-C₃ alkane fuels”. *Journal of Engineering for Gas Turbines and Power*.
- [13] Wang, H., and Sheen, D. A., 2015. “Combustion kinetic model uncertainty quantification, propagation and minimization”. *Progress in Energy and Combustion Science*, **47**, pp. 1–31.
- [14] Prager, J., Najm, H. N., Sargsyan, K., Safta, C., and Pitz, W. J., 2013. “Uncertainty quantification of reaction mechanisms accounting for correlations introduced by rate rules and fitted arrhenius parameters”. *Combustion and Flame*, **160**(9), pp. 1583–1593.
- [15] Turányi, T., and Tomlin, A. S., 2016. *Analysis of kinetic reaction mechanisms*. Springer, Berlin.
- [16] Sheen, D. A., and Wang, H., 2011. “The method of uncertainty quantification and minimization using polynomial chaos expansions”. *Combustion and Flame*, **158**(12), pp. 2358–2374.
- [17] Slavinskaya, N. A., Abbasi, M., Starcke, J. H., Whitside, R., Mirzayeva, A., Riedel, U., Li, W., Oreluk, J., Hegde, A., Packard, A., Frenklach, M., Gerasimov, G., and Shatalov, O., 2017. “Development of an uncertainty quantification predictive chemical reaction model for syngas combustion”. *Energy & Fuels*, **31**(3), pp. 2274–2297.
- [18] Frenklach, M., Wang, H., and Rabinowitz, M. J., 1992. “Optimization and analysis of large chemical kinetic mechanisms using the solution mapping method-combustion of methane”. *Progress in Energy and Combustion Science*, **18**(1), pp. 47–73.
- [19] Zsély, I. G., Zádor, J., and Turányi, T., 2008. “Uncertainty analysis of NO production during methane combustion”. *International Journal of Chemical Kinetics*, **40**(11), pp. 754–768.
- [20] Wiener, N., 1938. “The homogeneous chaos”. *American Journal of Mathematics*, **60**(4), pp. 897–936.
- [21] Reagan, M. T., Najm, H., Pebay, P., Knio, O., and Ghanem, R., 2005. “Quantifying uncertainty in chemical systems modeling”. *International journal of chemical kinetics*, **37**(6), pp. 368–382.
- [22] Lipardi, A. C., Bergthorson, J. M., and Bourque, G., 2016. “NO_x Emissions Modeling and Uncertainty From Exhaust-Gas-Diluted Flames”. *Journal of Engineering for Gas Turbines and Power*, **138**(5), p. 051506.
- [23] Lipardi, A. C., Versailles, P., Watson, G. M., Bourque, G., and Bergthorson, J. M., 2017. “Experimental and numerical study on NO_x formation in CH₄-air mixtures diluted with exhaust gas components”. *Combustion and Flame*, **179**, pp. 325–337.
- [24] Goodwin, D., Moffat, H., and Speth, R., 2016. Cantera: An object-oriented software toolkit for chemical kinetics, thermodynamics, and transport processes. <http://www.cantera.org>.
- [25] Adams, B., Bauman, L., Bohnhoff, W., Dalbey, K., Ebeida, M., Eddy, J., Eldred, M., Hough, P., Hu, K., Jakeman, J., Stephens, J., Swiler, L., Vigil, D., and Wildey, T., 2015. Dakota, a multilevel parallel object-oriented framework for design optimization, parameter estimation, uncertainty quantification, and sensitivity analysis: Version 6.0 user’s manual. Tech. rep., Sandia Technical Report SAND2014-4633.
- [26] Baulch, D., Cobos, C., Cox, R., Esser, C., Frank, P., Just, T., Kerr, J., Pilling, M., Troe, J., Walker, R., et al., 1992. “Evaluated kinetic data for combustion modelling”. *Journal of Physical and Chemical Reference Data*, **21**(3), pp. 411–734.
- [27] Baulch, D. L., 2005. “Evaluated kinetic data for combustion modeling : Supplement II”. *Journal of physical and chemical reference data*, **34**(3), pp. 757–1397.
- [28] Tsang, W., and Hampson, R., 1986. “Chemical kinetic data base for combustion chemistry. Part I. Methane and related compounds”. *Journal of Physical and Chemical Reference*

- Data*, **15**(3), pp. 1087–1279.
- [29] Askey, R., and Wilson, J. A., 1985. *Some basic hypergeometric orthogonal polynomials that generalize Jacobi polynomials*, Vol. 319. American Mathematical Society, Providence.
- [30] Tomlin, A. S., 2006. “The use of global uncertainty methods for the evaluation of combustion mechanisms”. *Reliability Engineering & System Safety*, **91**(10-11), pp. 1219–1231.
- [31] Xiu, D., 2010. *Numerical methods for stochastic computations: A spectral method approach*. Princeton university press, Princeton.
- [32] Smith, R., 2013. *Uncertainty Quantification: Theory, Implementation, and Applications*. Computational Science and Engineering. SIAM, Philadelphia.
- [33] Smolyak, S., 1963. “Quadrature and interpolation formulas for tensor products of certain classes of functions”. *Soviet Math. Dokl.*, **4**, pp. 240–243.
- [34] Smith, G. P., Golden, D. M., Frenklach, M., Moriarty, N. W., Eiteneer, B., Goldenberg, M., Bowman, C. T., Hanson, R. K., Song, S., Gardiner, W. C. J., Lissianski, V. V., and Qin, Z., 1999. GRI-Mech 3.0. http://www.me.berkeley.edu/gri_mech/.